POLITECNICO DI TORINO
Repository ISTITUZIONALE

Thermal Noise Compliant Synthesis of Linear Lumped Macromodels

Terms of use:

Publisher copyright

(Article begins on next page)

19 December 2025

Thermal noise compliant synthesis of linear lumped macromodels

Stefano Grivet-Talocia, *Senior Member, IEEE*, Gianni Signorini, Salvatore Bernardo Olivadese, Claudio Siviero, Pietro Brenner

Abstract—This paper addresses the synthesis of equivalent circuits from black box state-space macromodels, as produced by model order reduction or rational curve fitting schemes. The emphasis is here thermal noise compliance, intended as the guarantee that the produced netlists can be safely used in standard solvers of the SPICE class to perform thermal noise analysis, in addition to usual DC, AC, and transient simulations. Due to the fact that Signal to Noise (S/N) ratio is a key figure of merit in nearly all signal processing analog circuits, noise analysis is mandatory in design and verification of most analog and RF/mm-wave electronic applications. However, common macromodel synthesis approaches rely on components that do not (and cannot) have an associated thermal noise model, such as controlled sources or negative circuit elements. Therefore, macromodel-based noise analyses are generally not possible with currently available approaches. We propose a circuit realization derived from the classical resistance extraction synthesis, with suitable modifications for enhancing macromodel sparsity and efficiency. The resulting equivalent netlist, which is compatible with any standard circuit solver, is shown to produce exact noise characteristics, even if its elements are derived through a mathematical procedure, totally unrelated to the actual topology of the physical system under modeling. The procedure is validated by several examples.

Index Terms—Macromodeling, Passivity, State-space models, Noise, Vector Fitting, Scattering, Immittance

I. INTRODUCTION

Reduced-order behavioral macromodels are nowadays a common tool in electronic design and verification flows. In general terms, a macromodel aims at describing a complex system based on its input-output behavior, through a simplified description of the dominant dynamics that can be observed from its external interface ports. Reduced-order macromodels of various components in a system enable much faster system level numerical simulations with respect to detailed descriptions based on first principle or partial differential equation models, thus enabling automated design, verification, and optimization flows. The application fields where macromodeling has been and is successfully adopted range from signal and power integrity in electronics, power distribution systems, thermal analysis, till mechanical, naval, and aerospace structural modeling, to name a few [1]–[4].

Based on the native characterization through which the behavior of the system or component under analysis is known, two main different macromodeling strategies can be defined. The first approach, usually denoted as Model Order Reduction (MOR), derives a macromodel starting from an existing detailed large-scale model through a projection or approximation process [1], [2]. The starting large-scale model is often available from the spatial discretization of field equations in integral form (e.g., Partial Element Equivalent Circuit, PEEC) or differential form (e.g., via Finite Elements or Finite Differences). The second approach applies instead system identification or curve fitting techniques [5]–[8] to sampled system responses, in order to construct a behavioral model whose dynamics are able to reproduce the same outputs. The raw characterization is usually available in the frequency or time domain as a result of direct measurements or full-wave simulations. When applied to linear systems, both these approaches lead to macromodels that can be cast in a state-space form [9], [10]. This will be the starting point in this paper.

Once a state-space macromodel is available, it is necessary to cast it in a form that is suitable for system-level analysis. Very often, the designers that need to use the model are forced to adopt specific circuit solvers, typically of the SPICE class. It is therefore convenient to translate the macromodel equations into an equivalent circuit based on standard elementary components, so that it can be parsed and solved by a general purpose circuit solver. This conversion is typically denoted as macromodel synthesis. A few advanced commercial solvers allow a direct inclusion of state-space matrices in the definition of a multiport component, making macromodel synthesis unnecessary. However, this feature is not available in all solvers, and certainly not in freeware or legacy SPICE engines.

Many different types of synthesis and circuit solver interfaces have been proposed in the past. Most of these are targeted to fast transient analysis, leading to various alternative techniques with a varying degree of complexity and numerical efficiency. Among these, most common solutions include: direct translation of the state-space equations via interconnected dependent sources [4], pole/zero or pole/residue forms [11], and direct admittance stamping [12]–[14], which however may lead to negative components that may be rejected by some solvers. All above approaches may be acceptable to setup a transient circuit analysis. However, they generally fail in thermal noise analysis, which is the main subject of this paper.

With electrical noise analysis, we consider the evaluation of the spectral components of the thermal noise generated by the lossy elements in the system operating at a given

temperature [15]. Thermal fluctuations induce in fact electrical noise that is observed at the system interface ports, and that for many applications is very important to be accounted for the computation of overall noise budget. Examples are all kind of analog and RF small-signal processing applications implemented in System on Chip or System in Package typically found in mobile platforms, such as smartphones and tablets.

The basic mechanism for noise generation is modeled and implemented in practically all modern circuit solvers, in form of equivalent noise sources associated to each elementary resistor [15], [16]. Unfortunately, when a behavioral macromodel is synthesized as an equivalent circuit, the resulting circuit elements are not at all related to the actual physics and topology of the underlying system. They are mere circuit representations of mathematical equations. As a result, a thermal noise analysis of a synthesized behavioral macromodel using a standard circuit solver loses significance and generally leads to wrong results: the equivalent circuit is simply used outside its scope of validity. The main purpose of this work is in fact to provide a non-intrusive bridge between the macromodel and the solver, so that with no modifications to the solver engine, the solver will be able to extract correct noise information.

We define as noise-compliant synthesis a process that generates an equivalent circuit that, once processed by a thermal noise analysis in a standard circuit solver, will produce noise spectra that are consistent with the physical device under modeling. To the best of the Authors' knowledge, there is at present no commercial tool that is able to conduct a correct thermal noise analysis when a behavioral (state-space) macromodel is embedded in the simulation deck. We show however that there are several possibilities to achieve this goal. In particular, any circuit realization that uses only positive resistors, inductors, capacitors, and ideal transformers leads to a noise-compliant macromodel. We therefore see that any of the classical synthesis methods [17] such as Youla's reactance extraction [18] or Darlington and Belevitch synthesis [19], [20] will do, although these approaches have never been applied for behavioral macromodel synthesis. Two exceptions are [21], where a first attempt based on reactance extraction was documented, and [22], which provides an alternative approach based on classical spectral factorization. These earlier methods do not specifically address the sparsity and the efficiency of the resulting circuit when solved numerically. In fact, classical synthesis approaches were developed several decades ago to physically realize circuits, at that time of moderate complexity. However, the sparsity and the numerical efficiency of large-size macromodels with possibly thousands of states, as required by the complexity of modern components and systems, is very important and should be considered as a prerequisite for an effective macromodeling flow.

The main contribution of this work is a noise-compliant synthesis process that builds on Darlington's and Belevitch's idea of resistance extraction [12], [17], [20], and differently from [21], produces a sparse equivalent circuit whose complexity scales only linearly with the number of macromodel states n. As a result, the macromodel netlist can be seamlessly used in any type of circuit analysis such as AC, DC, TRAN (Transient), PSS (Periodic Steady State), HB (Harmonic Balance), and for all kinds of noise analysis with high efficiency. Moreover, differently from [22], the proposed method produces a netlist of basic circuit elements, that is compatible with any circuit solver. The excellent scalability of proposed synthesis is demonstrated on selected test cases from real designs.

II. BACKGROUND AND NOTATION

We consider a p-port macromodel with an immittance (impedance or admittance) or scattering transfer matrix $\mathbf{H}(s)$ defined by a state-space realization

$$\mathbf{H}(s) = \mathbf{D} + \mathbf{C}(s\mathbf{I} - \mathbf{A})^{-1}\mathbf{B} \leftrightarrow \left[\begin{array}{c|c} \mathbf{A} & \mathbf{B} \\ \hline \mathbf{C} & \mathbf{D} \end{array}\right], \quad (1)$$

with $\mathbf{A} \in \mathbb{R}^{n \times n}$, $\mathbf{B} \in \mathbb{R}^{n \times p}$, $\mathbf{C} \in \mathbb{R}^{p \times n}$, $\mathbf{D} \in \mathbb{R}^{p \times p}$, where s is the Laplace variable The realization is assumed to be minimal, i.e., both controllable and observable. Furthermore, the macromodel is stable, so that the eigenvalues of $\mathbf{A}$ have either negative real part or are purely imaginary with unit multiplicity. Several minimal realizations can be associated to the same macromodel through a similarity transformation

$$\mathbf{H}(s) \leftrightarrow \left[\begin{array}{c|c} \mathbf{A} & \mathbf{B} \\ \hline \mathbf{C} & \mathbf{D} \end{array}\right] \leftrightarrow \left[\begin{array}{c|c} \mathbf{TAT}^{-1} & \mathbf{TB} \\ \hline \mathbf{CT}^{-1} & \mathbf{D} \end{array}\right] \quad (2)$$

defined by any nonsingular matrix $\mathbf{T} \in \mathbb{R}^{n \times n}$. The macromodels considered in this work are passive and reciprocal. We review the corresponding definitions and conditions below [17], [23]–[25]. Passivity is achieved either by construction using one of the passivity-preserving MOR approaches [4], [26], or by direct enforcement [27]–[35].

A. Passivity

According to the input-output representation of the macromodel, we define

$$\boldsymbol{\Theta}(s) = \begin{cases} \frac{1}{2}(\mathbf{H}(s) + \mathbf{H}(s)^{\mathsf{H}}) & \text{immittance} \\ \mathbf{I} - \mathbf{H}(s)^{\mathsf{H}}\mathbf{H}(s) & \text{scattering} \end{cases} \quad (3)$$

where $^{\mathsf{H}}$ denotes conjugate (hermitian) transpose (we will denote transposition with $^{\mathsf{T}}$ and conjugation with *). The macromodel is passive if its transfer matrix $\mathbf{H}(s)$ is positive real (immittance) or bounded real (scattering), i.e., when the following three conditions hold

1) $\mathbf{H}(s^*) = \mathbf{H}^*(s)$;
2) $\mathbf{H}(s)$ has no singularities for $\text{Re}\{s\} > 0$;
3) $\boldsymbol{\Theta}(s) \geq 0$ for $\text{Re}\{s\} > 0$.

If these conditions hold and, in addition, $\boldsymbol{\Theta}(j\omega) = 0$ for each $\omega \in \mathbb{R}$ such that $j\omega$ is not a pole of $\mathbf{H}(s)$, then the system is lossless. Note that for scattering systems, condition 3 implies that $\mathbf{H}(s)$ is regular on the imaginary axis $s = j\omega$.

Equivalent conditions that characterize passive state-space systems are provided by the Positive Real Lemma (PRL)

$$\exists \mathbf{P} = \mathbf{P}^{\mathsf{T}} > 0: \quad \mathcal{P}(\mathbf{P}) \leq 0 \quad (4)$$

where

$$\mathcal{P}(\mathbf{P}) = \begin{bmatrix} \mathbf{A}^{\mathsf{T}}\mathbf{P} + \mathbf{PA} & \mathbf{PB} - \mathbf{C}^{\mathsf{T}} \\ \mathbf{B}^{\mathsf{T}}\mathbf{P} - \mathbf{C} & -(\mathbf{D} + \mathbf{D}^{\mathsf{T}}) \end{bmatrix} \quad (5)$$

which applies to immittance systems, and by the Bounded Real Lemma (BRL)

$$\exists \mathbf{P} = \mathbf{P}^\mathsf{T} > 0 : \quad \mathcal{B}(\mathbf{P}) \leq 0 \tag{6}$$

where

$$\mathcal{B}(\mathbf{P}) = \begin{bmatrix} \mathbf{A}^\mathsf{T}\mathbf{P} + \mathbf{P}\mathbf{A} + \mathbf{C}^\mathsf{T}\mathbf{C} & \mathbf{P}\mathbf{B} + \mathbf{C}^\mathsf{T}\mathbf{D} \\ \mathbf{B}^\mathsf{T}\mathbf{P} + \mathbf{D}^\mathsf{T}\mathbf{C} & -(\mathbf{I} - \mathbf{D}^\mathsf{T}\mathbf{D}) \end{bmatrix} \tag{7}$$

valid for scattering systems. Further, if the block matrices $\mathcal{P}(\mathbf{P}) = \mathbf{0}$ or $\mathcal{B}(\mathbf{P}) = \mathbf{0}$ in (5) and (7) for some symmetric and positive definite matrix $\mathbf{P}$, then the state-space realization defines a *lossless* system.

In case the inequalities (4) and (6) are satisfied by $\mathbf{P} = \mathbf{I}$, then the state-space realization is called *internally passive*. An internally passive realization $\{\bar{\mathbf{A}}, \bar{\mathbf{B}}, \bar{\mathbf{C}}, \bar{\mathbf{D}}\}$ can be obtained by any passive realization (1) by applying a similarity transformation (2) defined by any matrix $\mathbf{T}$ such that $\mathbf{P} = \mathbf{T}^\mathsf{T}\mathbf{T}$. Note that, even if some of the original state-space matrices are sparse, the resulting internally passive state matrices produced by this transformation are in general full. The computation of $\mathbf{P}$ can be performed by solving some associated Algebraic Riccati Equations [36] by one of the several available techniques [37]–[42].

B. Reciprocity

An immittance or scattering transfer matrix $\mathbf{H}(s)$ describes a reciprocal system if it is symmetric, $\mathbf{H}(s) = \mathbf{H}(s)^\mathsf{T}$. Applying this symmetry constraint to the state-space realization (1), we can easily obtain the following characterization of reciprocal state-space macromodels

$$\exists \mathbf{T} = \mathbf{T}^\mathsf{T} : \quad \mathbf{A}\mathbf{T} = \mathbf{T}\mathbf{A}^\mathsf{T}, \quad \mathbf{B} = \mathbf{T}\mathbf{C}^\mathsf{T}, \tag{8}$$

where $\mathbf{T}$ is nonsingular, complemented by the obvious condition $\mathbf{D} = \mathbf{D}^\mathsf{T}$. Suppose that a nonsingular symmetric matrix $\mathbf{T}$ is found such that (8) holds. Let us compute its eigendecomposition $\mathbf{T} = \mathbf{Q}\boldsymbol{\Lambda}\mathbf{Q}^\mathsf{T}$, where $\mathbf{Q}$ is orthogonal and $\boldsymbol{\Lambda} = \mathrm{diag}\{\lambda_i\}$, and let us define

$$\boldsymbol{\Sigma}_{\mathrm{int}} = \mathrm{diag}\{\mathrm{sgn}(\lambda_i)\}, \quad \mathbf{R} = \mathbf{Q}\,\mathrm{diag}\{\sqrt{|\lambda_i|}\}, \tag{9}$$

where sgn extracts the sign of its argument. Matrix $\boldsymbol{\Sigma}_{\mathrm{int}}$ is a diagonal of $+1$ and -1 and is called *internal signature matrix*. Applying the similarity transformation defined by matrix $\mathbf{R}^{-1}$ to the original state-space system, we obtain the new realization

$$\mathbf{H}(s) \leftrightarrow \left[\begin{array}{c|c} \mathbf{A}_{\mathrm{rec}} & \mathbf{B}_{\mathrm{rec}} \\ \hline \mathbf{C}_{\mathrm{rec}} & \mathbf{D}_{\mathrm{rec}} \end{array} \right] = \left[\begin{array}{c|c} \mathbf{R}^{-1}\mathbf{A}\mathbf{R} & \mathbf{R}^{-1}\mathbf{B} \\ \hline \mathbf{C}\mathbf{R} & \mathbf{D} \end{array} \right], \tag{10}$$

for which (8) becomes

$$\mathbf{A}_{\mathrm{rec}}\boldsymbol{\Sigma}_{\mathrm{int}} = \boldsymbol{\Sigma}_{\mathrm{int}}\mathbf{A}_{\mathrm{rec}}^\mathsf{T}, \quad \mathbf{B}_{\mathrm{rec}} = \boldsymbol{\Sigma}_{\mathrm{int}}\mathbf{C}_{\mathrm{rec}}^\mathsf{T}. \tag{11}$$

This latter property defines an *internally reciprocal* state-space realization.
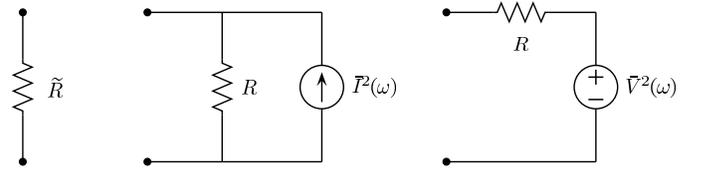

Fig. 1. Norton and Thevenin equivalent circuits for a noisy resistor $\widetilde{R}$.

III. NOISE COMPLIANCE

Consider a physical multiport linear circuit made of positive resistors, inductors, capacitors, and ideal transformers, henceforth denoted as physical RLCT network, and assume thermal equilibrium at a given temperature T. It is well known that the noise properties of the circuit can be derived by replacing each noisy resistor $\widetilde{R}$ with an equivalent Thevenin (Norton) local noise source, as depicted in Fig. 1, connected in series (parallel) with a noiseless resistance R [15] (henceforth, a tilde will be used to label noisy components) These equivalent noise sources are characterized by their (white) noise spectra $\bar{V}^2(\omega) = 4K_b T R$ or $\bar{I}^2(\omega) = 4K_b T G$, where $G = 1/R$ and $K_b = 1.38065 \times 10^{-23} J/K$ is the Boltzmann constant. The power spectral densities and cross-spectra of the noise that is observed at the circuit interface ports are simply derived by considering all internal noise sources as uncorrelated, and by performing a standard AC circuit analysis.

Thanks to Nyquist theorem, the noise characterization at the circuit interface ports is also directly available in terms of its transfer matrix. Depending on the input-output representation, and recalling definition (3), the full p-port noise power spectral density matrix (which collects on the main diagonal the power spectral densities of the noise signals at each port, and their respective cross spectra in its off-diagonal entries) reads [16]

$$\mathcal{C}(\omega) = 4K_b T \boldsymbol{\Theta}(\mathrm{j}\omega) . \tag{12}$$

This well known result states that it is not necessary to consider or disclose the internal structure of the system under modeling in order to capture noise statistics. The latter can be readily determined only based on the frequency responses.

Assume now that the physical structure of the system is not known, and that only a black-box state-space macromodel (1) is available. The result (12) leads to the following conclusions.

- Any state-space description of the system response embeds via (3) and (12) a correct representation of the thermal noise, as it appears at the external ports. Therefore, any state-space macromodel can be defined as *Externally Noise Compliant (ENC)*, in the sense that the noise power spectral density matrix $\mathcal{C}(\omega)$ is available from direct evaluation of (12).

- Any RLCT circuit realization (with nonnegative circuit elements) that is constructed from the state-space macromodel is such that, upon replacing each resistor with its equivalent noise circuit (Fig. 1), will lead to the correct external noise characterization (12) by standard circuit analysis. This can be regarded as a corollary of Nyquist theorem. We define such circuit realization as *Internally Noise Compliant (INC)*. Note that, even if the components used in the circuit synthesis are not related at all with the

topology and the structure of the physical system under modeling, the noise power spectral densities and cross-spectra will be correct, since all components used in the synthesis that are lossy (hence can act as noise sources), namely the positive resistors, do have an associated self-consistent noise model.

- A circuit realization that synthesizes a given state-space macromodel, and that includes either negative components (in particular resistors $R < 0$) or controlled sources (CS), is guaranteed to be ENC but is generally not INC. This is due to the fact that negative resistors and controlled sources are not equipped with a noise model. A brute-force AC circuit analysis with any given circuit solver will not be able to reproduce the noise contributions from such elements, and will produce incorrect noise power spectral densities and cross-spectra at the external interface ports.

The above considerations allow us to state that, in order to achieve an INC macromodel synthesis, we should make sure that all lossy components that are responsible for power dissipation (hence noise generation), are suitably represented by circuit elements that have an associated elementwise noise model. In other words, all losses must be captured by positive resistors. A sufficient condition to achieve this goal is to perform a RLCT synthesis (note that ideal transformers are lossless and do not contribute to noise generation). Therefore, all classical synthesis methods that are able to produce a physically realizable RLCT network will be INC, including Youla's reactance extraction [18], Darlington's synthesis [19] and Belevitch's synthesis [12]. These are not the only possible INC synthesis approaches, however. We will show in the following that controlled sources are actually allowed, as far as their overall subnetwork does not dissipate any power. This idea is in fact the key enabling factor for our proposed approach, which achieves INC by making use of controlled sources to reduce overall circuit complexity.

We should mention an alternative approach to INC synthesis, recently presented in [22]. In this work, the Authors derive a companion noise model through a spectral factorization process, that is able to reproduce the desired frequency-dependent power spectral density matrix (12). The latter is used to filter white uncorrelated noise sources, in order to construct equivalent noise sources to be suitably connected to the external ports of a standard synthesized noiseless macro-model. With respect to this method, our proposed technique has the following advantages:

- INC is attained by construction, thus avoiding the need of building a second state-space model for the synthesis of the equivalent noise sources;
- the dynamic order of the macromodel (hence the number of reactive elements) matches the state-space size, whereas [22] duplicates the number of states;
- there is no need to synthesize explicitly a set of individual white uncorrelated noise sources, since these are generated automatically by the circuit solver, acording to Fig. 1;
- the proposed netlist is based on standard circuit elements,

hence compatible with any circuit solver, whereas [22] only communicates the state space matrices to a specific solver [45], thus restricting compatibility.

IV. FORMULATION

Our proposed macromodel synthesis is based on the classical Darlington resistance extraction. The p-port state-space macromodel (1) is realized as a $(p+\rho)$-port lossless network, whose first p port provide the external interface, and last ρ ports are closed on positive noisy resistances, as depicted in Fig. 2. The system decomposition is reviewed in Sec. IV-A for the immittance case, and in Sec. IV-B for the scattering case. These decompositions are well known, see [17].

A. System decomposition, immittance case

Our starting point is here an immittance macromodel described by a passive state-space realization (1). In particular, we require that the state-space realization is internally passive, so that the PRL condition (4) is fulfilled with $\mathbf{P} = \mathbf{I}$. Since $\mathcal{P}(\mathbf{I}) = \mathcal{P}(\mathbf{I})^\mathsf{T} \le 0$, we can perform the following (minimum-rank) factorization according to [17]

$$\mathcal{P}(\mathbf{I}) = -\mathcal{M}\mathcal{M}^\mathsf{T}, \quad \mathcal{M}^\mathsf{T} = \begin{bmatrix} \mathbf{L}^\mathsf{T} & \mathbf{W} \end{bmatrix}, \quad (13)$$

where a block partition of $\mathcal{M} \in \mathbb{R}^{(n+p)\times\rho}$ is induced by the block size in (5), so that $\mathbf{L} \in \mathbb{R}^{n\times\rho}$ and $\mathbf{W} \in \mathbb{R}^{\rho\times p}$. Using these matrix factors, we construct the following extended $(p+\rho)$-port state-space system

$$\mathbf{H}_L(s) \leftrightarrow \left[\begin{array}{c|c} \mathbf{A}_L & \mathbf{B}_L \\ \hline \mathbf{C}_L & \mathbf{D}_L \end{array} \right], \quad (14)$$

where

$$\mathbf{A}_L = \frac{1}{2}(\mathbf{A} - \mathbf{A}^\mathsf{T}) \quad (15a)$$

$$\mathbf{B}_L = \mathbf{C}_L^\mathsf{T} = \begin{bmatrix} \frac{1}{2}(\mathbf{B} + \mathbf{C}^\mathsf{T}) & \frac{-1}{\sqrt{2}}\mathbf{L} \end{bmatrix} \quad (15b)$$

$$\mathbf{D}_L = \begin{bmatrix} \frac{1}{2}(\mathbf{D} - \mathbf{D}^\mathsf{T}) & \frac{1}{\sqrt{2}}\mathbf{W}^\mathsf{T} \\ \frac{-1}{\sqrt{2}}\mathbf{W} & \mathbf{0} \end{bmatrix}. \quad (15c)$$

It is straightforward to see that
1) the immittance system $\mathbf{H}_L(s)$ is lossless, since its state-space matrices (15) satisfy the PRL condition (4) with an equality sign (and with $\mathbf{P} = \mathbf{I}$);
2) closing the last ρ ports of $\mathbf{H}_L(s)$ into unit resistances leads to a p-port system described by the original transfer matrix $\mathbf{H}(s)$ of the macromodel (1).

The above system decomposition complies with the structure depicted in Fig. 2. The smallest allowed number of resistors ρ equals the normal rank of $\mathbf{H}(s) + \mathbf{H}(-s)^\mathsf{T}$, so that $\rho \le p$.

B. System decomposition, scattering case

The same steps for immittance system decomposition discussed in Sec. IV-A can be repeated for the scattering case, with simple modifications. The starting point is always an internally passive state-space realization such that the BRL condition (6) is fulfilled with $\mathbf{P} = \mathbf{I}$. Applying to $\mathcal{B}(\mathbf{I})$ the
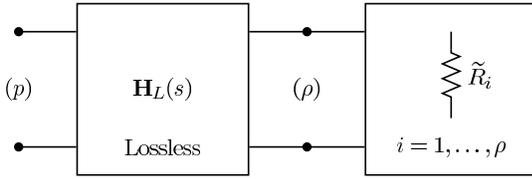
Fig. 2.   System decomposition through resistance extraction.

same factorization (13) allows us to construct a lossless system (14) with (scattering) transfer matrix $\mathbf{H}_L(s)$, characterized by state-space matrices

$$\mathbf{A}_L = \mathbf{A} \tag{16a}$$

$$\mathbf{B}_L = \begin{bmatrix} \mathbf{B} & -(\mathbf{C}^\mathsf{T}\mathbf{D}_{12} + \mathbf{L}\mathbf{D}_{22}) \end{bmatrix} \tag{16b}$$

$$\mathbf{C}_L^\mathsf{T} = \begin{bmatrix} \mathbf{C}^\mathsf{T} & \mathbf{L} \end{bmatrix} \tag{16c}$$

$$\mathbf{D}_L = \begin{bmatrix} \mathbf{D} & \mathbf{D}_{12} \\ \mathbf{W} & \mathbf{D}_{22} \end{bmatrix}, \tag{16d}$$

where the last ρ columns of $\mathbf{D}_L$ formed by $\mathbf{D}_{12}$ and $\mathbf{D}_{22}$ are constructed to form an orthonormal basis of the subspace that is orthogonal to the first p columns, implying that $\mathbf{D}_L^\mathsf{T}\mathbf{D}_L = \mathbf{I}$. As for the immittance case, it is straightforward to verify that

1) the scattering system $\mathbf{H}_L(s)$ is lossless, since its state-space matrices (16) satisfy the BRL condition (6) with an equality sign (and with $\mathbf{P} = \mathbf{I}$);
2) closing the last ρ ports of $\mathbf{H}_L(s)$ into resistances $\widetilde{R}_0$ (equal to the normalization impedance that defines the adopted scattering representation), leads to a p-port system described by the original transfer matrix $\mathbf{H}(s)$ of the macromodel (1).

Therefore, we see that also this decomposition complies with the structure depicted in Fig. 2. Also in this case we have that the smallest possible ρ equals the normal rank of $\mathbf{I} - \mathbf{H}(-s)^\mathsf{T}\mathbf{H}(s)$, so that $\rho \leq p$.

C. Some remarks

The system decomposition carried out in Sec. IV-A and Sec. IV-B, respectively, for immittance and scattering representations, leads to a state-space description of the lossless coupling system $\mathbf{H}_L(s)$. The macromodel synthesis is therefore complete once we are able to produce an equivalent circuit for this lossless system. It turns out that $\mathbf{H}_L(s)$ is generally not symmetric, or equivalently, the state-space realizations (15) and (16) do not satisfy conditions (8). This implies that the lossless system is not guaranteed to be reciprocal, even if the original macromodel (1) is reciprocal.

Lack of reciprocity of $\mathbf{H}_L(s)$ may seem a dead end, since it is well known that a RLCT synthesis of nonreciprocal networks is impossible, and at least gyrators if not controlled sources are needed. In fact, most research efforts that led to the most prominent classical synthesis approaches have been targeted to purely reciprocal syntheses without gyrators. In the context of synthesis from state-space description, the fundamental requirement for achieving a purely reciprocal synthesis is to obtain a particular state-space realization that is at the same time internally passive and internally reciprocal. If

the underlying system is passive and reciprocal, this is indeed always possible, as discussed in [17], [24]. Such a realization enables purely reciprocal synthesis by both resistance and reactance extraction, even addressing additional constraints such as minimality in the number of reactive or resistive elements. It is however unfortunate that all these purely reciprocal techniques require extensive use of ideal transformer networks (or multport transformers), whose size is essentially dictated by the model order n. As a consequence, the number of equivalent elementary (scalar) components that are produced in the synthesis scales as $O(n^2)$, as shown in [21]. We can regard this fact as a consequence that internally passive and reciprocal state-space realizations are generally characterized by full matrices.

Our main objective in this work is not a synthesis based on individually passive and reciprocal components. Rather, we want to guarantee noise compliance and sparsity. The price we will have to pay to achieve a sparse synthesis is in fact a relaxation of the reciprocity constraint. Therefore, the fact that $\mathbf{H}_L(s)$ is not symmetric has no importance in our context, as far as we can produce for it a sparse circuit representation that is noise compliant. We should remark that, if we start from a reciprocal macromodel $\mathbf{H}(s) = \mathbf{H}(s)^\mathsf{T}$, the resulting overall circuit synthesis will be reciprocal at the external interface ports, since the decompositions of Sec. IV-A and Sec. IV-B are exact, at least up to the numerical accuracy that is permitted by finite-precision arithmetics.

D. Sparse quasi-diagonal lossless realization

We start here from the state-space realization of $\mathbf{H}_L(s)$ defined by (15) or (16). In case all eigenvalues λ_i of $\mathbf{A}_L$ are simple, or at least with a geometric multiplicity that equals their algebraic multiplicity, we can perform a full diagonalization

$$\mathbf{T}_c^{-1}\mathbf{A}_L\mathbf{T}_c = \mathbf{\Lambda}_c = \mathrm{diag}\{\lambda_i\}, \tag{17}$$

where $\mathbf{T}_c$ collects the eigenvectors and is in general complex-valued. Since $\mathbf{A}_L$ is real, however, a straightforward manipulation [43] applied to each pair of complex conjugate eigenvalues $\lambda_i = \alpha_i \pm \mathrm{j}\beta_i$ and corresponding eigenvectors leads to the real block-diagonal form

$$\mathbf{T}^{-1}\mathbf{A}_L\mathbf{T} = \mathbf{\Lambda} = \mathrm{blkdiag}\left\{\ldots, \mu_i, \ldots, \mathbf{\Lambda}_i, \ldots\right\}, \tag{18}$$

where μ_i denote the purely real eigenvalues and

$$\mathbf{\Lambda}_i = \begin{bmatrix} \alpha_i & \beta_i \\ -\beta_i & \alpha_i \end{bmatrix}. \tag{19}$$

We remark that in the immittance case $\mathbf{A}_L$ is skew-symmetric, so that α_i and μ_i must be identically vanishing. For the scattering case, instead, the eigenvalues of $\mathbf{A}_L$ are equal to the poles of the initial macromodel. In both cases, the nonvanishing entries in $\mathbf{\Lambda}$ are at most n.

When the state-space matrix $\mathbf{A}_L$ is defective, it cannot be diagonalized since there does not exist a complete basis of eigenvectors. Since the Jordan decomposition is well-known to be ill-conditioned and unreliable [43], we resort to a more

numerically stable decomposition based on a block-diagonal Schur factorization. This is defined as

$$\mathbf{T}^{-1}\mathbf{A}_L\mathbf{T} = \mathbf{\Lambda} = \text{blkdiag}\left\{\ldots, \mu_i, \ldots, \mathbf{\Lambda}_i, \ldots, \mathbf{S}_i, \ldots\right\}. \quad (20)$$

where μ_i and $\mathbf{\Lambda}_i$ collect simple eigenvalues or multiple eigenvalues with complete eigenspaces, with the corresponding eigenvectors stacked in the respective columns of $\mathbf{T}$. Each of the blocks $\mathbf{S}_i$ arises instead from a partial Schur decomposition of the contribution from a defective Jordan block (which is never formed explicitly). A corresponding orthogonal basis is constructed and placed in $\mathbf{T}$. The construction of (20) is available from function `bdschur` in the MATLAB software [44]. Also in this case, the number of nonvanishing coefficients in $\mathbf{\Lambda}$ is $O(n)$ due to the very unlikely occurrence of large-size defective eigenspaces.

Application of the above constructed similarity transformation $\mathbf{T}^{-1}$ to the realization $\{\mathbf{A}_L, \mathbf{B}_L, \mathbf{C}_L, \mathbf{D}_L\}$ leads to a diagonal or almost-diagonal realization of the lossless coupling network

$$\mathbf{H}_L(s) \leftrightarrow \left[\begin{array}{c|c} \mathbf{\Lambda} & \hat{\mathbf{B}}_L \\ \hline \hat{\mathbf{C}}_L & \mathbf{D}_L \end{array}\right] = \left[\begin{array}{c|c} \mathbf{T}^{-1}\mathbf{A}_L\mathbf{T} & \mathbf{T}^{-1}\mathbf{B}_L \\ \hline \mathbf{C}_L\mathbf{T} & \mathbf{D}_L \end{array}\right], \quad (21)$$

where the number of nonvanishing coefficients is $O((2p + 2\rho + 1)n + (p + \rho)^2)$, whereas the corresponding complexity of realizations (15) or (16) is $O(n^2 + (2p + 2\rho)n + (p + \rho)^2)$. Since typically $n \gg p \geq \rho$, the overall complexity is greatly reduced.

E. Sparse lossless coupling network synthesis

The state-space system (21) is cast in expanded form as

$$\dot{x}_i(t) = \sum_j \Lambda_{ij} x_j(t) + \sum_j \hat{B}_{L,ij} u_j(t), \quad (22)$$

$$y_k(t) = \sum_j \hat{C}_{L,kj} x_j(t) + \sum_j D_{L,kj} u_j(t), \quad (23)$$

where inputs and outputs are $u_j = \{v_j, i_j, a_j\}$ and $y_j = \{i_j, v_j, b_j\}$ for admittance, impedance, and scattering representations, respectively.[1] Its synthesis is performed here in the simplest and most direct way, according to [4]. Both state and output equations are constructed as the interconnection of Controlled Sources (CS), as depicted in Fig. 3. Summations are realized as series or parallel connections of elementary controlled sources, in order to guarantee compatibility with all possible circuit solvers. All components are considered as "cold" or noiseless, including the auxiliary resistance R_0 that is needed for the realization of the scattering output equation. This synthesis will be denoted as RCCS since based only on Resistors, Capacitors, and Controlled Sources.

As already stated in Sec. IV-A and Sec. IV-B, the last ρ ports are closed on unit resistances $\widetilde{R}_i = 1\Omega$ for immittance representations, and on reference resistances $\widetilde{R}_0$ for scattering representations. These termination resistors are defined as "noisy", so that a noise analysis performed by a standard

[1]The adopted scattering representation is based on power incident waves $a_j = (\sqrt{2R_0})^{-1}(v_j + R_0 i_j)$ and reflected waves $b_j = (\sqrt{2R_0})^{-1}(v_j - R_0 i_j)$, normalized to a positive real resistance R_0.
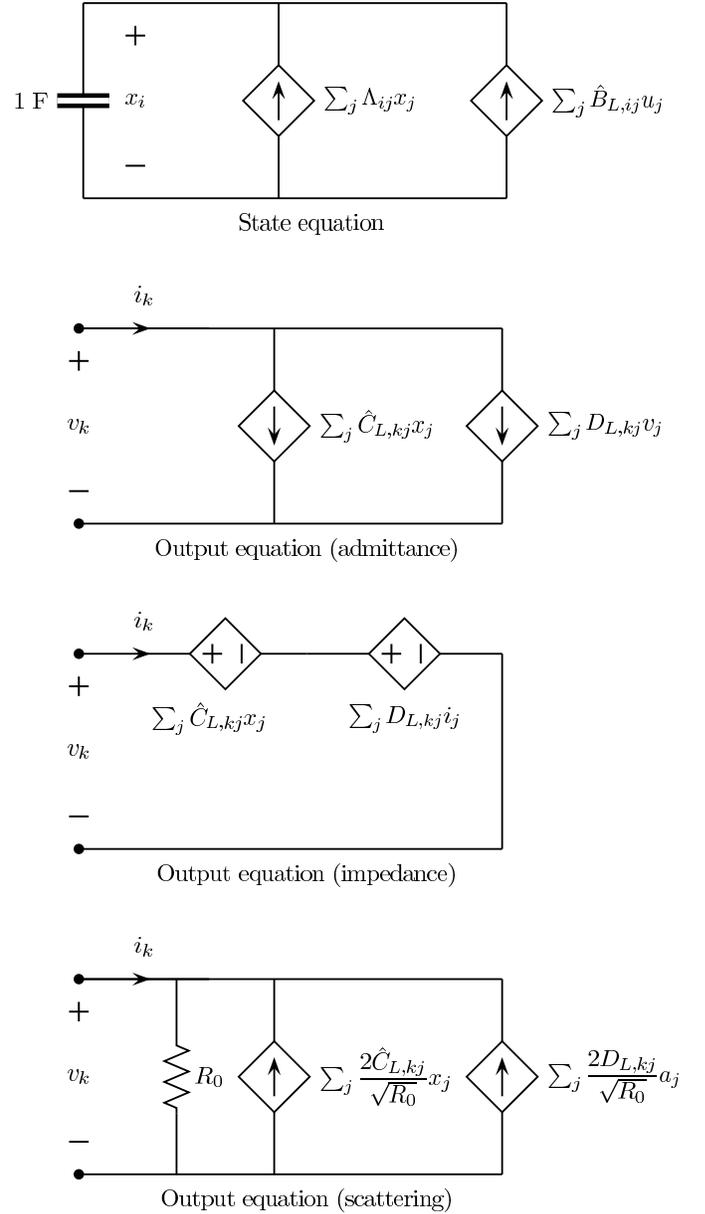

Fig. 3. RCCS synthesis of lossless coupling network $\mathbf{H}_L(s)$. In the state equation synthesis, input $u_k = \{v_k, i_k, a_k\}$ for admittance, impedance, and scattering cases, respectively.

circuit solver will replace them with the equivalent circuit depicted in Fig. 1. Internal Noise Compliance of this synthesis is guaranteed, since $\mathbf{H}_L(s)$ is lossless, and since all components used in its realization are defined as noiseless.

We should remark that some modern circuit solvers allow a direct implementation of multiport elements described by state-space matrices. An example is the component `cktrom` in Cadence Spectre [45]. Since these components are generally considered as noiseless by the simulators, the synthesis of $\mathbf{H}_L(s)$ can also be performed by just communicating to the solver its state-space matrices (15) or (16). Internal Noise Compliance will be guaranteed also with this simpler approach, which is however not general and solver-dependent.

TABLE I
NUMBER OF NODES AND CIRCUIT ELEMENTS IN THE SYNTHESIZED
EQUIVALENT CIRCUITS OF THE LC TANK CORE MACROMODEL. LAST ROW
REPORTS THE SIMULATION TIME REQUIRED FOR COMPUTING
S-PARAMETERS.

order: 350 ports: 25	RCCS	Reactance extraction	Resistance extraction
nodes	400	1406	475
C	350	177	350
L	—	173	—
R	350	293	75
CS	9925	106732	35498
time	20s	10min	1min

V. EXAMPLES

The proposed equivalent circuit synthesis technique has been verified on a large number of test cases. Here, we report the results for two state-space models derived from real designs in Sec. V-A and Sec. V-B. For these two cases, consistency is verified through a reference solution, obtained by defining a set of noise sources with spectral densities specified by (12), which are then suitably connected to the state-space system defining the multiport macromodel under analysis (assumed noiseless). The resulting system is then solved analytically at each frequency point through a Matlab script. The corresponding results will be labeled as "data" in all plots.

Noise compliance and network size of proposed synthesis will be compared to three alternative approaches, one based on direct state-space synthesis through controlled sources, and the other two based on reactance extraction [21] and spectral factorization [22]. It should be considered that [22] suggests no circuit synthesis, but proposes to communicate directly to the solver [45] the state-space matrices of the macromodels (through the cktrom component). We will see that, although the adopted state-space realizations are quasi-diagonal and sparse, the achieved runtime for [22] is much larger than for proposed approach.

The good scalability properties of proposed approach is finally documented in Sec. V-C, where the network complexity of the various synthesis methods is compared as a function of model order n and port count p.

A. LC-tank core of a Digitally Controlled Oscillator

The first example is based on a state-space model for a centrally involved LC-tank core from an Digitally Controlled RF Oscillator (DCO) containing a coil structure, capacitor feed lines and other interconnects, see Fig. 4. DCO's can be accurately tuned by means of digital controls: the noise behavior is a key figure of merit and therefore requires accurate noise modeling of all the parts in the design. In particular, the structure under modeling includes the metal lines of the tank core, the VDD and VSS supply lines, excluding the MOS transistors and the array of capacitors. A total of $p = 25$ ports were placed at the device pins and at the ends of the supply lines. The interconnect parasitics were extracted by means of field solver [46] in form of tabulated frequency responses (S-parameters).
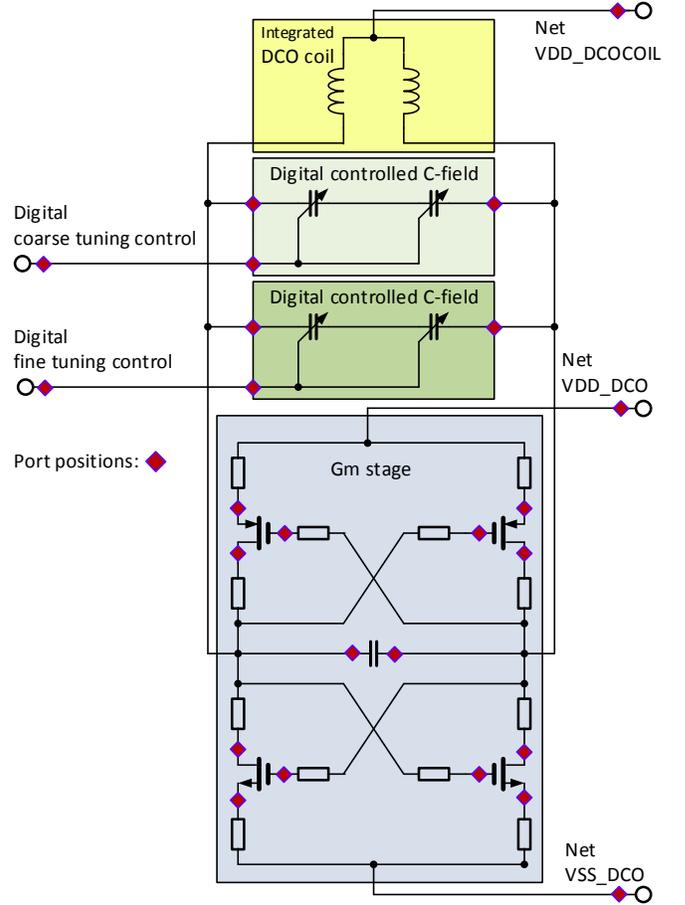

Fig. 4. Schematic illustration of a Digitally Controlled Oscillator.

A passive and reciprocal black-box macromodel (order $n = 350$) was first obtained by rational fitting [5], followed by passivity enforcement as implemented in [27], [28]. The model, available in pole-residue form, was then processed to compute a Gilbert quasi-diagonal state-space realization [10], [47], which was then synthesized into a RCCS equivalent network as in Sec. IV-E without any preliminary resistance extraction. The resulting circuit is not INC. Then, three different INC syntheses were carried out, based on reactance extraction [21], on spectral factorization [22], and on the new proposed resistance extraction.

The scattering responses computed from SPICE via AC sweeps of the INC synthesized networks are compared to the reference in Fig. 5. As expected, all synthesis approaches provide the same result. The voltage noise (port 1) spectral densities computed by standard SPICE noise analyses are reported in Fig. 6. We see that the noise spectral density is correctly reproduced only by the INC synthesized networks, whereas the direct RCCS synthesis gives incorrect results.

The number of circuit elements for each of the synthesized circuits (except [22], which is not comparable) is reported in Table I. The table shows that the RCCS synthesis is the most compact (but not INC). The other two INC circuits have more circuit elements, but the proposed approach is significantly less complex, since it preserves the same dynamic order of the
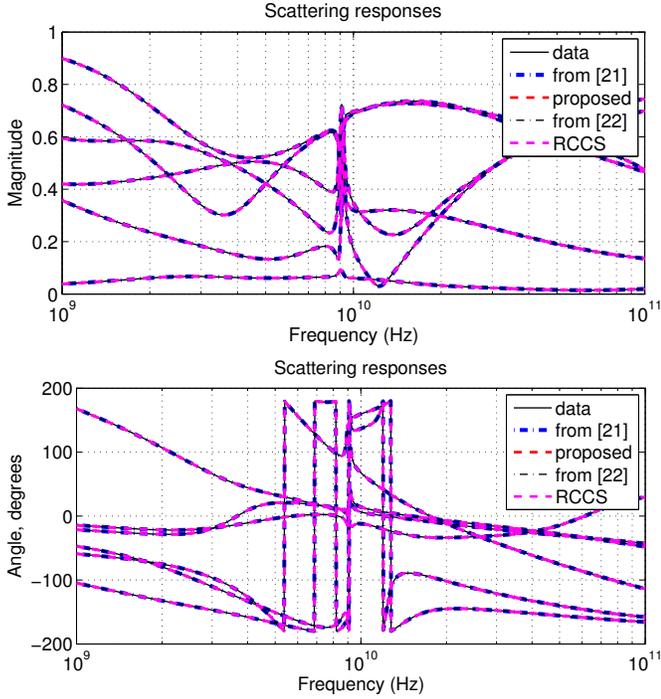
Fig. 5. Scattering responses for the LC-tank core example. Comparison between reference (thin black solid line) and synthesized macromodel via reactance extraction (blue dash-dotted line), proposed resistance extraction (red dashed line), spectral factorization (black dash-dotted line), and standard RCCS (dashed purple line).

Fig. 7. Scattering responses of the frontend SAW filter. Comparison between reference (thin black solid line) and synthesized macromodel via reactance extraction (blue dash-dotted line), proposed resistance extraction (red dashed line), spectral factorization (black dash-dotted line), and standard RCCS (dashed purple line).
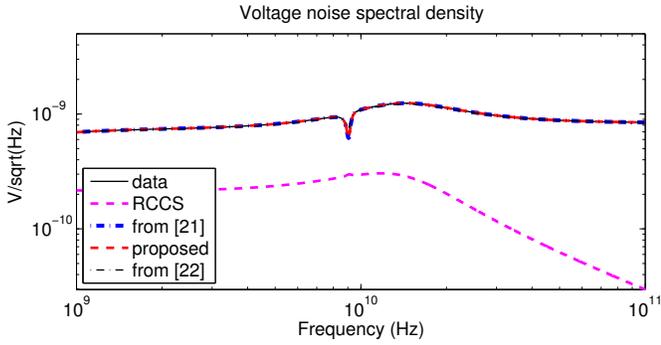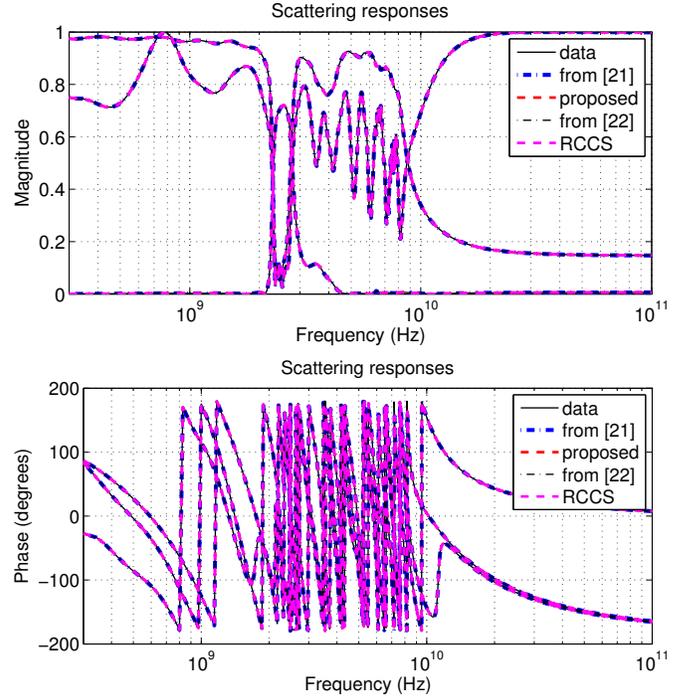

Fig. 6. Noise analysis results for the LC-tank core example. Results from reactance extraction (blue dash-dotted line), spectral factorization (black dash-dotted line), and proposed resistance extraction (red dashed line) match with the reference (thin black line), whereas the direct RCCS synthesis (dashed purple line) is not noise compliant.
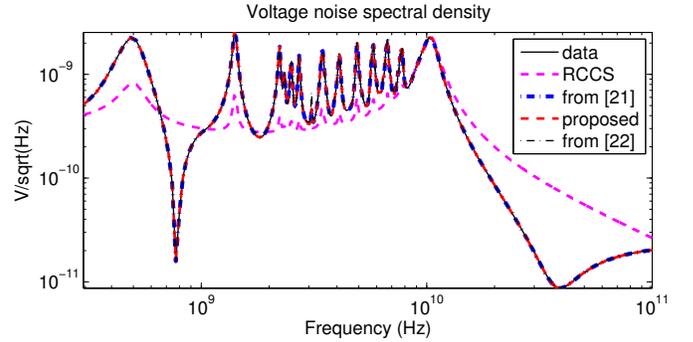

Fig. 8. Noise analysis results for the frontend SAW filter example. Results from reactance extraction (blue dash-dotted line), spectral factorization (black dash-dotted line) and proposed resistance extraction (red dashed line) match with the reference (thin black line), whereas the direct RCCS synthesis (dashed purple line) is not noise compliant.

model, with a minimal overhead in the number of nodes. The number of controlled sources used in the synthesis (directly related to matrix fill-in in the solver), is about three times less than for reactance extraction.

The total runtime required by an AC sweep for the evaluation of the Scattering responses of the synthesized macromodel over $K = 3500$ points is reported in the last row of Table I. Our proposed equivalent circuit runs about 10 times faster than the corresponding circuit from reactance extraction, with an overhead of about $3\times$ with respect to the RCCS netlist. The netlist from [22] performed the same analysis in a runtime of 9.5 minutes, comparable to the reactance extraction case.

B. Frontend SAW filter

The second example we consider is a $p = 2$ port frontend SAW filter design used in the receiver chain of a 3G transceiver. Also in this case noise compliance is of paramount importance. In fact, all components in a receiver chain are carefully designed and optimized in order to minimize noise contributions and signal distortion of the weak signal from the antenna. The basic component under study is the GP6 Dual SAW filter, whose scattering responses were measured and processed by the same modeling flow already discussed in Sec. V-A for the LC tank core structure, obtaining a state-space macromodel with order $n = 248$.

TABLE II
NUMBER OF NODES AND CIRCUIT ELEMENTS IN THE SYNTHESIZED
EQUIVALENT CIRCUITS OF THE FRONTEND SAW FILTER MACROMODEL.
LAST ROW REPORTS THE SIMULATION TIME REQUIRED FOR COMPUTING
S-PARAMETERS.

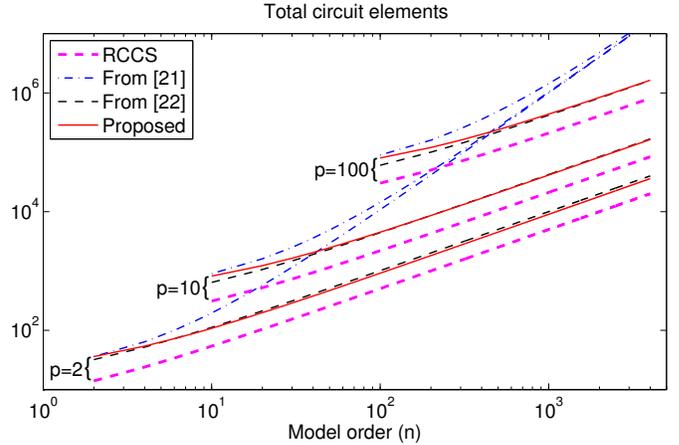| order: 248 ports: 2	RCCS	Reactance extraction	Resistance extraction
nodes	252	869	258
C	248	124	248
L	—	124	—
R	248	493	6
CS	874	42206	1980
time	0.5s	1min	1.2s

Fig. 9.   Total number of circuit elements for RCCS, reactance extraction, and proposed resistance extraction synthesis, reported as a function of model order n and number of interface ports p.

The accuracy of the scattering responses of the INC synthesized networks is confirmed by Figure 7. The (port 1) voltage noise spectral density as computed by SPICE through a noise analysis is reported for the four different synthesized networks in Fig. 8. Also in this case, the three INC networks provide consistent spectra, whereas the results based on the RCCS synthesis is completely wrong.

Since the ratio n/p between model order and number of ports is larger for this example with respect to the LC tank core case, we expect a more dramatic enhancement in circuit sparsity for our proposed approach with respect to the reactance extraction synthesis [21]. This is demonstrated in Table II. The total number of circuit elements from proposed approach is only slightly larger than for the RCCS synthesis but significantly smaller than from the reactance extraction synthesis. As a result, the total runtime required for an AC sweep (last row in Table II) demonstrates a speedup of $50\times$ with respect to the reactance extraction case, but only a moderate overhead of $2.4\times$ with respect to the RCCS case. The synthesis from [22] required for the same analysis a very long total runtime of 1 minute and 52 seconds, even if a quasi-diagonal state-space realization was used.

C. Scalability analysis

In this section, we compare the network complexity of the RCCS, reactance extraction [21], spectral factorization [22], and proposed resistance extraction syntheses. Since [22] does not suggest a circuit synthesis, but communicates directly to the solver [45] the state-space matrices of the macromodel, instead of network complexity (number of circuit elements) we report for [22] the total number of nonvanishing entries in the state-space models. We further assume that the macromodel has a quasi-diagonal state-space realization as presented in Section IV-D, although this detail is not discussed in [22]. Therefore, the results that are reported for [22] should be regarded as a best case, characterized by the least possible complexity among all possible state-space realizations.

Figure 9 reports the total number of components (or nonzero state matrix elements) required by the four different syntheses with varying order n and port count p, under the assumption that $\mathbf{A}_L$ can be diagonalized, and assuming that $\rho = p$, i.e., the normal rank of $\mathbf{H}(s) + \mathbf{H}(-s)^{\mathsf{T}}$ (immittance case) or $\mathbf{I} - \mathbf{H}(-s)^{\mathsf{T}}\mathbf{H}(s)$ (scattering case) is maximum. We see that our proposed approach is most efficient when $n \gg p$, i.e.,

when the dynamic order is much larger than the interface ports (the most common scenario in many applications). If $p \lesssim n$, the proposed synthesis is less sparse due to the presence of many controlled sources in the input-to-state and state-to-output maps $\mathbf{B}_L$ and $\mathbf{C}_L$ of the lossless coupling network, and the complexity of all four syntheses becomes comparable. For large n, both proposed approach, [22] (with a quasi-diagonal realization), and the RCCS synthesis scale as $O(n)$, whereas the reactance extraction synthesis scales as $O(n^2)$.

We remark that all documented synthesis approaches produce equivalent circuits with a minimum number n of reactive elements (states), except [22], which requires $2n$ internal states. The proposed resistance extraction approach also attains the least possible number of resistors ρ. The reactance extraction requires instead a larger number of resistors due to the additional constraints (internal reciprocity) required by the synthesis process [17], and further requires a large number of ideal transformers, here realized by a pair of controlled sources.

VI. CONCLUSIONS

This paper presented a systematic approach for the equivalent circuit synthesis of behavioral linear lumped macromodels. The key feature of proposed approach is the thermal noise compliance of the synthesized circuit, intended as the ability of the network to provide consistent power spectral densities of thermal noise from internal resistive losses. This is guaranteed even if the realized network is just a mere translation into a behavioral circuit of the macromodel state-space matrices, which have no direct relationship with the topology of the physical structure that the macromodel is intended to represent. The proposed approach produces a unique equivalent network that can be safely used in DC, AC, transient (TRAN), and all kind of noise analyses using off the shelf SPICE solvers.

REFERENCES

[1] A.C. Antoulas, *Approximation of large-scale dynamical systems*, SIAM, Philadelphia, 2005.

[2] W.H.A. Schilders, H.A. Van Der Vorst, and J. Rommes, *Model order reduction: theory, research aspects and applications*, Springer Verlag, 2008.

[3] M. Nakhla and R. Achar, "Simulation of High-Speed Interconnects", *Proc. IEEE*, May 2001, Vol. 89, No. 5, pp. 693–728.

[4] M. Celik, L. Pileggi, A. Odabasioglu, *IC Interconnect Analysis*, Springer, 2002.

[5] B. Gustavsen, A. Semlyen, "Rational approximation of frequency domain responses by vector fitting", *IEEE Trans. Power Del.*, vol. 14, no. 3, pp. 1052-1061, July, 1999.

[6] D. Deschrijver, B. Haegeman, T. Dhaene, "Orthonormal Vector Fitting: A Robust Macromodeling Tool for Rational Approximation of Frequency Domain Responses," *IEEE Trans. Adv. Packaging*, vol. 30, pp. 216–225, May 2007.

[7] S. Grivet-Talocia, "Package macromodeling via Time-Domain Vector Fitting," *IEEE Microwave Wireless Comp. Lett.*, Vol. 13, No. 11, 2003.

[8] D. Deschrijver, M. Mrozowski, T. Dhaene, D. De Zutter, "Macromodeling of Multiport Systems Using a Fast Implementation of the Vector Fitting Method," *IEEE Microwave and Wireless Components Letters*, Vol. 18, N. 6, June 2008, pp.383–385.

[9] R.E. Kalman, "Mathematical description of linear dynamical systems", *SIAM Journal on Control*, vol. 1, no. 2, pp. 152-192, 1963.

[10] T. Kailath, *Linear systems*, Prentice-Hall Englewood Cliffs, NJ, 1980.

[11] R. Foster, "A reactance theorem", *Bell System Journal*, Tech. Rep., 1924.

[12] V. Belevitch, *Classical network theory*, Holden-Day, 1968.

[13] Z. Qi, H. Yu, P. Liu, S.X.Tan, L. He, "Wideband passive multiport model order reduction and realization of RLCM circuits," *IEEE Trans. on Computer-Aided Design of Integrated Circuits and Systems*, vol. 25, no. 8, pp. 1496–1509, Aug. 2006

[14] G. Antonini, "SPICE equivalent circuits of frequency-domain responses," *IEEE Trans. on Electromagnetic Compatibility*, vol. 45, no. 3, pp. 502–512, Aug. 2003

[15] H. Nyquist, "Thermal agitation of electricl charge in conductors", *Physical Review*, vol. 32, pp. 110–113, July 1928

[16] R. Q. Twiss, "Nyquists and Thevenins theorems generalized for nonreciprocal linear networks," *J. Appl. Phys.*, vol. 26, no. 5, pp. 599602, 1955

[17] B.D.O. Anderson, S. Vongpanitlerd, *Network Analysis and Synthesis*, Prentice Hall, Englewood Cliff, 1973.

[18] D.C. Youla and P. Tissi, "n-Port Synthesis via Reactance Extraction - Part I", in *IEEE Int. Conv., New York, NY, 1966*, pp. 183-207.

[19] S. Darlington, "Synthesis of reactance 4-poles which produce prescribed insertion loss characteristics, including special applications to filter design", PhD thesis, Columbia university, 1940.

[20] B.D.O. Anderson, R. Brockett, "A Multiport State-Space Darlington Synthesis," *IEEE Trans. on Circuit Theory*, vol. 14, no. 3, pp. 336–337, Sept.1967

[21] S. B. Olivadese, S. Grivet-Talocia, P. Brenner, "Noise compliant macromodel synthesis for RF and Mixed-Signal applications" , *IEEE 22nd Conference on Electrical Performance of Electronic Packaging and Systems*, San Jose (CA) USA, pp. 129-132, October 27-30, 2013.

[22] Z. Ye, "Noise Companion State-Space Passive Macromodeling for RF/mm-Wave Circuit Design", in *IEEE Trans. Comput.-Aided Des. Integr. Circuits Syst.*, vol. 32, no. 9, pp. 1435-1440, Sept. 2013.

[23] P. Triverio, S. Grivet-Talocia, M.S. Nakhla, F. Canavero, R. Achar, "Stability, causality, and passivity in electrical interconnect models", *IEEE Trans. on Advanced Packaging*, vol. 30, no. 4, pp. 795-808, 2007.

[24] T. Reis, J.C. Willems, "A balancing approach to the realization of systems with internal passivity and reciprocity", in *System e Control Letters*, vol. 60, pp. 69-74, Elsevier, 2011.

[25] S. Boyd, L. El Ghaoui, E. Feron and V. Blakrishnan, *Linear Matrix Inequalities in System and Control Theory*, SIAM Studies in Applied Mathematics, vol. 15, SIAM, 1994.

[26] J.R.Phillips, L.Daniel, L.M. Silveira, "Guaranteed passive balancing transformations for model order reduction," *IEEE Trans. Computer-Aided Design of Integrated Circuits and Systems*, vol. 22, no. 8, pp. 1027–1041, Aug. 2003.

[27] S. Grivet-Talocia, "Passivity Enforcement via Perturbation of Hamiltonian Matrices" , in *IEEE Trans. Circuits and Systems I: Fundamental Theory and Applications*, pp. 1755-1769, vol. 51, n. 9, September, 2004.

[28] S. Grivet-Talocia, "An Adaptive Sampling Technique for Passivity Characterization and Enforcement of Large Interconnect Macromodels", in *IEEE Trans. on Advanced Packaging*, vol. 30, n. 2, pp. 226-237, May, 2007.

[29] C. P. Coelho, J. Phillips, L. M. Silveira, "A Convex Programming Approach for Generating Guaranteed Passive Approximations to Tabulated Frequency-Data", *IEEE Trans. Computed-Aided Design of Integrated Circuits and Systems*, Vol. 23, No. 2, pp. 293–301, Feb. 2004.

[30] D. Saraswat, R. Achar and M. Nakhla, "Global Passivity Enforcement Algorithm for Macromodels of Interconnect Subnetworks Characterized by Tabulated Data", *IEEE Transactions on VLSI Systems*, Vol. 13, No. 7, pp. 819–832, July 2005.

[31] B. Gustavsen, A. Semlyen, "Enforcing passivity for admittance matrices approximated by rational functions", *IEEE Trans. Power Systems*, Vol. 16, N. 1, pp. 97–104, Feb. 2001.

[32] S. Grivet-Talocia, A. Ubolli, "Passivity Enforcement With Relative Error Control" , *IEEE Trans. Microwave Theory and Techniques*, Vol. 55, No. 11, pp. 2374–2383, Nov. 2007.

[33] C. S. Saunders, Jie Hu, C. E. Christoffersen, M. B. Steer, "Inverse Singular Value Method for Enforcing Passivity in Reduced-Order Models of Distributed Structures for Transient and Steady-State Simulation, " *IEEE Trans. Microwave Theory and Techniques*, Vol. 59, No. 4, pp. 837–847, Apr. 2011.

[34] S. Grivet-Talocia and A. Ubolli, "A comparative study of passivity enforcement schemes for linear lumped macromodels," *IEEE Trans. Advanced Packaging*, vol. 31, pp. 673–683, Nov 2008.

[35] G.C. Calafiore, A.Chinea, S.Grivet-Talocia, "Subgradient Techniques for Passivity Enforcement of Linear Device and Interconnect Macromodels," *IEEE Trans. on Microwave Theory and Techniques*, vol. 60, no. 10, pp. 2990–3003, Oct. 2012

[36] P. Lancaster, L. Rodman, *Algebraic Riccati Equations*, Oxford University Press, 1995.

[37] D. Bini, B. Iannazzo, B. Meini, *Numerical Solution of Algebraic Riccati Equations*, SIAM Fundamentals of Algorithms, n.9, 2012.

[38] A.J. Laub, "A Schur method for solving Algebraic Riccati Equations", *IEEE Transactions on Automatic Control*, vol. 24, n. 6, pp. 913-921, Dec. 1979.

[39] D. Kleinman, "On an iterative technique for Riccati equation computations", *IEEE Transactions on Automatic Control*, vol. 13, n. 1, pp. 114-115, Feb. 1968.

[40] S. Hammarling, "Newton's method for solving the Algebraic Riccati Equation", NPL Report DICT 12/82, National Physical Laboratory, Teddington, Middlesex TW11 0LW, UK, 1982.

[41] P. Benner and R. Byers, "An Exact Line Search Method for Solving Generalized Continuous-Time Algebraic Riccati Equations", *IEEE Transactions on Automatic Control*, vol. 43, no. 1, Jan. 1998, pp. 101–107.

[42] N. Sadegh, J.D. Finney, B.S. Heck, "An explicit method for computing the positive real lemma matrices", *International Journal of Robust and Nonlinear Control*, Vol. 7, no. 12, pp. 1057–1069, 1997.

[43] G. H. Golub, C.F. Van Loan, *Matrix computations*, 3rd ed., Baltimore: John Hopkins University Press, 1996.

[44] *Matlab User Guide*, The Mathworks Inc., 2012.

[45] *Virtuoso Spectre Circuit Simulator Reference*. Cadence Design Systems, 2007

[46] *HFSS*. Ansys, Inc., 2011.

[47] R. Achar, M. Nakhla, "Minimum realization of reduced-order high-speed interconnect macromodels", in *Signal Propagation on Interconnects*, H. Grabinski and P. Nordholz Eds., Kluwer, 1998.

Stefano Grivet-Talocia (M'98–SM'07) received the Laurea and the Ph.D. degrees in electronic engineering from Politecnico di Torino, Italy. From 1994 to 1996, he was with the NASA/Goddard Space Flight Center, Greenbelt, MD, USA. Currently, he is an Associate Professor of Circuit Theory with Politecnico di Torino. His research interests are in passive macromodeling of lumped and distributed interconnect structures, model order reduction, modeling and simulation of fields, circuits, and their interaction, wavelets, time-frequency transforms, and their applications. He is author of more than 120 journal and conference papers. He is co-recipient of the 2007 Best Paper Award of the IEEE Trans. Advanced Packaging. He received the IBM Shared University Research (SUR) Award in 2007, 2008 and 2009. Dr. Grivet-Talocia served as Associate Editor for the IEEE Transactions on Electromagnetic Compatibility from 1999 to 2001. He is co-founder and President of IdemWorks.

Gianni Signorini was born in Volterra (Pisa, Italy) in 1987. He received the BSc (2010) and MSc (magna cum laude, 2012) in Electronic Engineering from the University of Pisa, where he is currently pursuing a Ph.D in Information Engineering. Since 2011, he is with Intel Corporation, Munich (Germany), where he performs his research activity in the field of Signal and Power Integrity for high-speed PHYs in mobile SoCs.

Pietro Brenner was born in Dillingen, Germany in 1965. He received the Master degree in physics from the TUM (Munich) in 1993. From 1994 to 1996 he was a Research Assistant at the Fraunhofer Institute for Atmospheric Environmental Research (IFU), Germany, where he was working on the development of a mobile LIDAR ozone and aerosol measurement system.

In 1996 he joined Siemens Semiconductors, now Infineon Technologies (IFX) where he has been working for seven years on characterization and modeling of RF-BiCMOS technologies. Main focus was in that time the development of geometry-scalable RF-device characterization and modeling methodology for integrated active and passive RF-devices. A secondary field of activity was the development of enhanced test structures for fast on-wafer device characterization and improvement of parameter extraction methodology.

In 2003 he moved to IFX Analog & RF simulation methodology where he was working on analog behavioral modeling and simulation methodology. His general research interest was the development of application-specific behavioral circuit block models and application of model-based simulation methods for analog-, RF- and mixed signal designs (SoC's & SiP's).

In 2011 he moved to Intels Product Engineering Group (PEG) where he currently works in a central AMS & RF Design Flow and Methodology group. Focus of his work is simulation-based performance verification to enable pre-tapeout Crosstalk, IR-Drop, Power and Signal Integrity verification. He is there the responsible methodology expert for crosstalk prevention measures to be applied in design of Mobil Transceiver and Connectivity SoCs.

His general research interest are physics-based modelling approaches and complexity reduction methods (MOR) to enable accurate performance simulation also for complex designs. Pietro Brenner has published several journal and conference publications, many workshop presentations, and owns 3 invention disclosures.

Salvatore Bernardo Olivadese received the Laurea degree (B.Sc) in Information Technology in 2007, the Laurea Specialistica degree (M.Sc) in Electronic Engineering in 2009 and the Ph.D. in Electronic Engineering in 2014, all from Politecnico di Torino, Italy. For his bachelor thesis He developed a Web 2.0 service for scientific parallel applications, and for his master thesis He spent 6 months as visiting researcher at the Interconnect and Packaging Analysis Group of IBM T.J. Watson Research Center, Yorktown, NY, developing an Adaptive Frequency Sampling method. He was recipient of the IBM PhD Fellowship Award for the academic year 2011/12. His research interests concern packaging, circuit theory, Signal and Power Integrity, and parallel algorithms. Part of this research was conducted in collaboration with IBM, Intel, and IdemWorks.

Claudio Siviero received his Diploma in electrical engineering in 2003 and his Ph.D. degree in 2007 from the Politecnico di Torino, Italy, where he is now a research assistant with the Electromagnetic Compatibility group. From 2008 to 2013 he was with the IBM Development in Boeblingen, Germany, working as electronic packaging engineer. His research interests concern macromodeling of electrical interconnects for Electromagnetic Compatibility and Signal Integrity problems. In particular, he works on algorithms development for optimization and order reduction of large-scale dynamical systems and on behavioral modeling of nonlinear circuit elements, with specific application to the characterization of digital integrated circuits.